

# Visuo-Tactile Pretraining for Cable Plugging

Abraham George<sup>1</sup>, Selam Gano<sup>1</sup>, Pranav Katragadda<sup>1</sup>, and Amir Barati Farimani<sup>1</sup>

**Abstract**—Tactile information is a critical tool for fine-grain manipulation. As humans, we rely heavily on tactile information to understand objects in our environments and how to interact with them. We use touch not only to perform manipulation tasks but also to learn how to perform these tasks. Therefore, to create robotic agents that can learn to complete manipulation tasks at a human or super-human level of performance, we need to properly incorporate tactile information into both skill execution and skill learning. In this paper, we investigate how we can incorporate tactile information into imitation learning platforms to improve performance on complex tasks. To do this, we tackle the challenge of plugging in a USB cable, a dexterous manipulation task that relies on fine-grain visuo-tactile serving. By incorporating tactile information into imitation learning frameworks, we are able to train a robotic agent to plug in a USB cable - a first for imitation learning. Additionally, we explore how tactile information can be used to train non-tactile agents through a contrastive-loss pretraining process. Our results show that by pretraining with tactile information, the performance of a non-tactile agent can be significantly improved, reaching a level on par with visuo-tactile agents. For demonstration videos and access to our codebase, see the project website: <https://sites.google.com/andrew.cmu.edu/visuo-tactile-cable-plugging/home>

## I. INTRODUCTION

Achieving proficiency in complex manipulation tasks remains a longstanding challenge in robotics, with applications ranging from industrial automation to clay sculpting [1], [2]. Critical to addressing this challenge is the integration of tactile information, which provides both an understanding of the objects being interacted with and a detailed feedback response for closed-loop control. As humans, we instinctively rely on tactile feedback to navigate and manipulate objects with precision, leveraging sensory cues to modulate grip force, detect surface textures, and discern subtle changes in object properties [3]. In addition to using this tactile information to complete tasks, we also rely heavily on our tactile perception to learn manipulation skills [4].

In the realm of robotics, replicating this nuanced interplay between touch and manipulation is an ongoing field of research. Recent advancements in tactile sensing technologies, pioneered by devices such as GelSight [5], have enabled the incorporation of complex tactile information in robotic control pipelines. Prior works have used this tactile information to complete a wide range of manipulation tasks, such as cable routing, object detection, peg insertion, and door opening [6]–[9]. In these works, tactile information was incorporated into a wide range of control policies, including classical control, reinforcement learning, and imitation learning.

<sup>1</sup>With the Department of Mechanical Engineering, Carnegie Mellon University {aigeorge, selamg, pkatraga, afariman}@andrew.cmu.edu

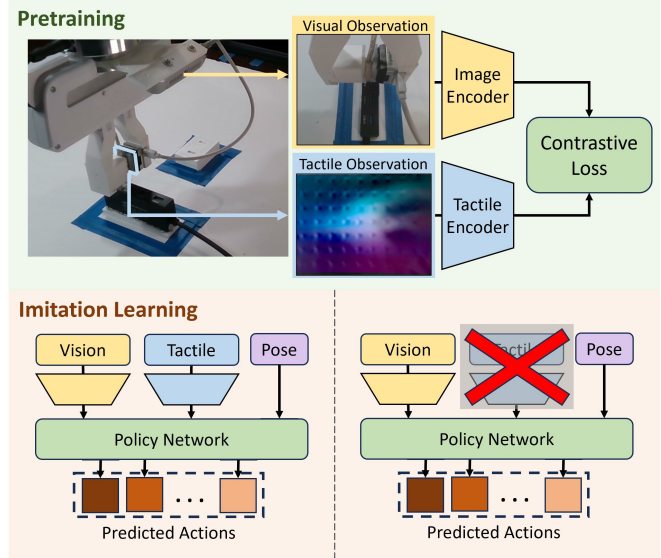


Fig. 1. Diagram of our approach. First, an image encoder and a tactile encoder are pretrained on the collected demonstrations using a temporally informed multi-modal contrastive loss. Then, the pretrained encoders are used in an imitation learning framework, either for visuo-tactile control (left) or vision-only control (right).

In this paper, we build upon these prior works, integrating tactile information into two imitation learning frameworks: Action Chunking Transformers (ACT) [10] and Diffusion Policy [11]. Our primary contribution is a pretraining strategy for these SOTA imitation learning frameworks, leveraging the multimodal nature of our data to incorporate a temporal-based visual-tactile contrastive-loss pretraining step.

In this step, a tactile encoder and an image encoder are trained to project their respective input modalities onto a shared latent space, with the goal of producing similar embeddings from multi-modal observations of the same scene. This task forces the encoders to learn the relationship between visual and tactile observations and to emphasize features present in both modalities - primarily contact-related features - which are important for dexterous manipulation. In the first use case we explore, these pretrained encoders are used as the observation backbone in a visuo-tactile imitation learning framework, allowing the agent to better leverage existing multi-modal relationships within its visuo-tactile training dataset. In the second use case, we discard the tactile encoder and use the pretrained vision encoder as the backbone for a vision-only imitation learning framework. By pretraining a vision-only policy with the multi-modal dataset, the policy can leverage an implicit tactile understanding

without requiring tactile information during deployment.

To evaluate our visuo-tactile imitation learning framework, we trained ACT and Diffusion Policy agents to plug in a USB cable - a challenging high-precision variant of peg insertion. Our experiments show that multi-modal pretraining moderately improves the performance of visuo-tactile imitation learning policies, and significantly improves vision-only policies, allowing them to achieve performance comparable to visuo-tactile agents.

## II. RELATED WORKS

### A. Tactile Sensing in Robotics

Tactile sensing has become widely recognized as a crucial component in robotic manipulation, with a wide range of tactile sensors proposed in recent years [12], measuring touch through normal forces [13], [14], tangential forces [15]–[17], contact torque [18], [19], vibration [20], [21], thermal contact [22], [23], and object proximity [24], [25]. This wide range of sensors has been used to tackle a variety of tasks, including object localization [26]–[28], object classification [7], [29], [30], dynamics detection [31], [32], and control tasks [9]. This paper will focus on the application of visual-tactile deformation-tracking sensors, specifically the GelSight Mini [5], for the task of cable plugging. This family of tactile sensors, which includes devices such as GelSight [5], Densetact [33]–[35], and See-Through-Your-Skin [36], work by tracking the displacement of a deformable contact material (usually silicon gel) to determine the strains applied during contact [37]. In the case of the GelSight Mini, a camera provides an RGB image of the underside of the silicon pad, which is illuminated by directional colored lighting. This lighting scheme allows for measuring the surface normal of the gel pad based on color, which can then be used to calculate a depth map (strain in  $z$ ) of the gel surface. The surface is also covered by a  $7 \times 9$  grid of tracking markers (black dots), whose displacement can be used to determine the tangential strain of the gel.

### B. Learning Control Policies using Tactile Sensors

Many prior works have sought to use tactile sensors to develop control policies, either through classical control, reinforcement learning, or imitation learning. [38], [39] combined classical control and heuristic approaches to tackle the problem of cable following and inserting wires. [6] went further, combining an LQR cable tracking controller with a fix-position headphone jack and a heuristic-based plugging controller to plug in a headphone cable. Moving beyond hardcoded policies, [40]–[42] combined visual and tactile observations to train RL agents to complete a range of tasks, including peg insertion, pick and place, and door opening. Although these works result in impressive policies, they require large amounts of training ( $\sim 1$  million steps) which can only be done in simulation. To avoid this computation intensity, a common strategy is to use Nearest Neighbors Imitation Learning [43], in which observations are compared to demonstrations via distance in an encoded latent space, and the demonstration which is nearest to the observation is

mimicked. [44] used this strategy, in combination with an RL residual policy, to learn visuo-tactile peg-insertion, and [8] used it to learn a variety of manipulation tasks including bowl unstacking, book opening, and joystick movement. Although VINN shows good performance with surprisingly little data, it lacks the ability to generalize and underperforms more robust direct action-prediction policies such as Action Chunking Transformers (ACT) [10].

### C. Contrastive Pretraining

Contrastive pretraining is a strategy to learn from unused aspects of data by training a model to associate like pairs of data and disassociate unlike pairs, usually by constructing a shared latent space [45]. This type of pretraining has been used in a wide range of fields from image classification [46], to symbolic regression [47], to molecular property prediction [48], to modeling partial differential equations [49]. Contrastive pretraining is especially useful for multi-modal datasets, where different modalities of the same observation, such as an image and a text caption of that image, can be paired [50]. In the field of visuo-tactile robotic systems, contrastive pretraining has been used to directly link vision and tactile observations, for example in identifying garment flaws [51]. Additionally, contrastive pretraining has been used to improve few-shot learning of visuo-tactile object classification [52], [53].

### D. Imitation Learning for Robotic Manipulation

Imitation learning casts the control problem as a supervised learning task: given a set of observation action pairs, train an agent to fit goal actions to given observations [54]. This method of control has been used for tasks ranging from automobile operation [55], to biped locomotion [56], to robotic manipulation tasks from block stacking [57] to kitchen chores [58]. However, imitation learning struggles with complex action spaces, non-deterministic goal policies, and significant shifts between training and testing (deployment) distributions [59]. Multiple solutions have been proposed to address these concerns, but we focus on two: Action Chunking Transformers (ACT) which use temporal ensembling to limit the effect of out-of-distribution actions, and Diffusion Policy, which uses diffusion to model complex action distributions.

1) *Action Chunking Transformers*: Action Chunking Transformers (ACT) [10] train a Conditional Variational Auto Encoder (CVAE) built upon a transformer backbone to predict a series of actions (in the form of goal positions) conditioned on state observations (position + vision). The use of an autoencoder for this task helps to reduce the negative effects of multi-modal distributions in the training data, as the latent variable can encode the "style" of the goal action sequence (ie. move left or move right). At inference time the latent variable is set to the mean of the prior (zero) to generate the most-likely action. The use of a strong KL divergence term in the loss function encourages the network to avoid over-reliance on the latent variable.

Because ACT predicts a sequence of actions (goal states),  $A_{t,t}$  to  $A_{t,t+h}$  at each timestep, during inference a series of previous predictions  $A_{t-h,t}$  to  $A_{t-1,t}$  is available. To reduce the effect of a single bad prediction (often caused by out-of-distribution states), this series of predictions is combined using a weighted average with exponentially decaying weights,  $w_i = e^{-ki}$ , and the resulting ensembled action is executed.

2) *Diffusion Policy*: To address the challenge of complex multi-modal action spaces, Diffusion Policy formulates visuomotor policies as Denoising Diffusion Probabilistic Models (DDPM) [60]. Such models iteratively denoise sets of observation-action pairs from a sample of Gaussian noise [61]. For a sample of Gaussian noise  $\mathbf{x}^k$ , a standard DDPM iteratively denoises for  $k$  steps with decreasing noise,  $\mathbf{x}^{k-1}, \mathbf{x}^{k-2}, \dots, \mathbf{x}^0$ , to generate noise-free output  $\mathbf{x}^0$ :

$$\mathbf{x}^{k-1} = \alpha(\mathbf{x}^k - \gamma\epsilon_\theta(\mathbf{x}^k, k) + \mathcal{N}(0, \sigma^2 I))$$

where  $\epsilon_\theta$  is the noise prediction network with learned parameters  $\theta$ , and  $\alpha, \gamma$ , and  $\sigma$  are parameters representing the noise schedule. At each iteration  $k$ , Gaussian noise  $\mathcal{N}(0, \sigma^2 I)$  is added.

Recent work by Chi and Feng et al [11] constructs a diffusion framework to generate action sequences conditioned on observations,  $p(\mathbf{O}_t | \mathbf{A}_t)$ , where  $\mathbf{O}_t$  is the observation at timestep  $t$  that action sequence  $\mathbf{A}_t$  is conditioned on. During training, a sample of unmodified examples,  $\mathbf{A}_t^0$ , is drawn from the dataset.

A random noise  $\epsilon^k$  is sampled with appropriate variance for denoising iteration step  $k$ . The noise prediction network  $\epsilon_\theta$  predicts the noise from the noised example data [11] using the following loss function:

$$Loss = MSE(\epsilon^k, \epsilon_\theta(\mathbf{O}_t, \mathbf{A}_t^0 + \epsilon^k, k))$$

In this case, the DDPM iteratively denoises a Gaussian sample representing the action sequence:

$$\mathbf{A}_t^{k-1} = \alpha(\mathbf{A}_t^k - \gamma\epsilon_\theta(\mathbf{O}_t, \mathbf{A}_t^k, k) + \mathcal{N}(0, \sigma^2 I))$$

The observation  $\mathbf{O}_t$  is used to condition the denoising process via Feature-Wise Linear Modulation (FiLM) layers in the noise prediction network, which enable a conditioning encoder to influence the network computation. [11], [62].

The training and inference noise scheduler are decoupled, allowing fewer denoising iterations during inference to improve speed. At inference,  $k_{infer}$  total iterations of denoising are performed to produce a noise-free action  $\mathbf{A}_t$ , and a greater number of  $k_{train}$  total iterations are used during training.

Other prior works applying diffusion to trajectory planning insert it as different components of reinforcement learning pipelines [63] or as data augmentation for reinforcement learning [64], [65].

### III. METHODS

#### A. Pretraining

In our approach to visuo-tactile robotic control, the agent has access to three data modalities: visual information (from cameras), tactile information (from a tactile sensor), and positional information (from proprioception). Each modality of data contributes a separate piece of information about the observed scene. For our control policy to successfully choose actions, it must have a rich understanding of the environment, incorporating knowledge from all three sources to form a single, cohesive observation. To instill an understanding of the relationships between the sources of data, we implemented a CLIP-inspired contrastive-loss pretraining strategy [46]. We trained two encoders, each using a separate modality, to produce latent representations of the scene. By optimizing the encoders to maximize the cross-modality dot-product similarity of latent representations from the same scene while minimizing the cross-modality similarity of latent representations from different scenes, we were able to instill the relationships between the separate modalities into our model. A diagram illustrating our pretraining strategy can be found in Figure 2, and the detailed implementation can be seen in Algorithm 1.

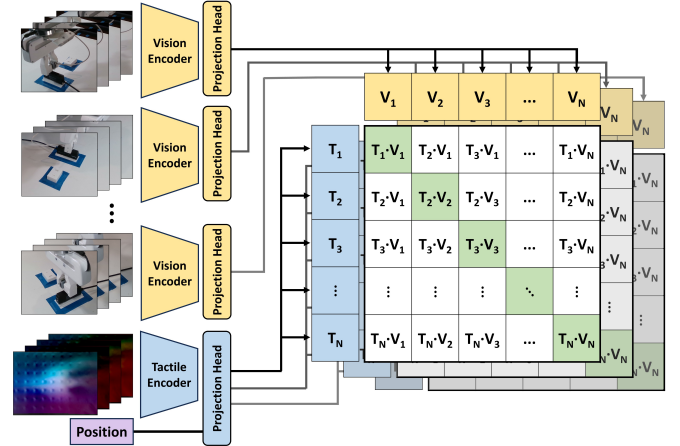


Fig. 2. Contrastive loss visualization. A series of visual observations  $V_1, V_2, \dots, V_N$  and tactile observations  $T_1, T_2, \dots, T_N$  are collected, and the vision encoder and tactile encoder are trained to make the embeddings from the same timestep similar while forcing apart the embeddings from different time steps.

To ensure that both encoders have a complete representation of the scene, we combined the tactile observations (which only contain local information) with the position observations (which only encode global information). Each encoder consists of a ResNet-18 [66] backbone, topped with a fully connected MLP layer to project the ResNet encoding to a 512 embedding space. In the tactile encoder, the positional information was also passed into the MLP projection head.

To form the contrastive pairs for the pretraining, we sampled  $n$  (we used 7) observations randomly from a single

---

**Algorithm 1** Contrastive Pretraining
 

---

**Input:**  $\{V\}, \{T\}, \{P\} \triangleright$  Vision, Tactile, and Position Obs

**Initialize:**  $E_V, E_T \triangleright$  Vision Encoder, Tactile Encoder

**while** Training **do**

  Sample Trajectory  $V, T, P$ , from set of observations

  Sample  $t = \{t_1, t_2, \dots, t_n\}$ , st.  $|t_i - t_j| > \Delta t_{min} \forall i, j$

**for**  $i \in t$  **do**

$latent\_T_i = E_T(T_i, P_i)$

**for**  $c$  in cameras **do**

$latent\_V_{i,c} = E_V(V_{i,c})$

**end for**

**end for**

$sim_{i,j,c} = ||latent\_T_i|| \bullet ||latent\_V_{j,c}|| \triangleright$  Similarity

$SM1_{i,c} = \frac{\exp(sim_{i,i,c}/\tau)}{\sum_{j \in t} \exp(sim_{i,j,c}/\tau)} \triangleright$  Softmax of  $sim$

$SM2_{i,c} = \frac{\exp(sim_{i,i,c}/\tau)}{\sum_{j \in t} \exp(sim_{j,i,c}/\tau)} \triangleright$  Softmax, other axis

$loss = -\sum_c \sum_{i \in t} \frac{1}{2n} (\log(SM1_{i,c}) + \log(SM2_{i,c}))$

  Update  $E_V$  and  $E_T$  using  $loss$

**end while**

---

demonstration, with the requirement that the samples must be at least  $\Delta t_{min}$  time steps (we used 10, which equates to 1 second) apart. By only sampling observation pairs from a single trajectory, and ensuring they are sufficiently separated in time and separated by time, this approach additionally instilled previously unused temporal information into the encoder, as the model had to learn how the scene changed over time, rather than in between runs.

For each timestep, we have multiple visual observations, one from each camera. During training, the contrastive loss between tactile and visual embeddings is calculated separately for each camera observation, and the resulting losses are combined and used to update the network. This strategy helps ensure balanced training of the vision encoder, which is shared across all cameras. Additionally, by enforcing similarity between the tactile embedding and each vision embedding for a given timestep, we implicitly align the embeddings of different views of the same scene. By having the cameras share an aligned latent space, we encourage the vision embedding to learn general features of the scene, rather than camera-specific characteristics.

### B. Imitation Learning Frameworks

We implemented two imitation learning frameworks to study the impact of tactile information on learning the dexterous manipulation of cable plugging: Action Chunking Transformer (ACT) [10] and Diffusion Policy [11]. A diagram of our two implementations can be seen in Figure 3.

1) *ACT: Action Chunking Transformer:* The primary imitation learning framework we used was an Action Chunking Transformer (ACT). We made two main modifications to the ACT framework. First, we replaced the stock Resnet vision encoder with the vision encoder from our contrastive pretraining and added a separate tactile encoder (also from our pretraining), to encode the tactile observations. The

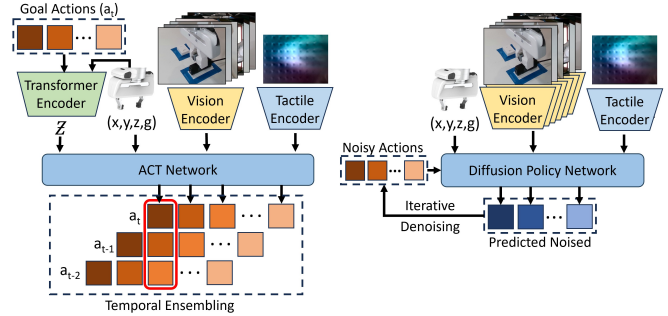


Fig. 3. Imitation learning networks. ACT (left) is trained as an autoencoder, predicting a sequence of actions at each timestep ( $a_t$ ). At inference, the latent variable,  $z$ , is set to 0. The network is queried each timestep, and all action predictions for that timestep are ensembled using a weighted average. Diffusion Policy (right) learns to predict noise applied to an action sequence. During inference, the action sequence is initialized with Gaussian noise and is iteratively denoised to produce output actions.

tactile encoding is concatenated with the vision encodings before being passed into ACT’s transformer decoder. Second, instead of training the network to predict goal positions, we trained it to predict relative goal positions ( $goal\_pos_{t,t:t+h} - pos_{t,t}$  instead of  $goal\_pos_{t,t:t+h}$ ). At inference, we add the current position to the predictions to get goal positions in the global coordinate frame. Operating in the delta position space, instead of the position space, allows the network to avoid biases that would be detrimental to the task of visual-servoing. At inference, we used standard temporal ensembling, in the global coordinate frame, with a temperature constant of  $k = 0.25$ .

2) *Diffusion Policy:* Our approach to diffusion leveraged the recent work by Chi and Feng et. al. that generates action sequences conditioned on observations with DDPM [11]. We use the CNN-based implementation of this model, where a 1D temporal CNN models the conditional action distribution.

For this approach, each observation (visual, tactile, and positional) is passed through an encoder, and the resulting embeddings are stacked to form a single observation vector. For vision observations, we replace the stock ResNet18 encoder with our pre-trained encoder (with separately fine-tuned, identically initialized encoders for each camera view). For tactile observations, we use our pre-trained tactile encoder. The network then uses the observation embedding vector to condition its noise prediction.

We use an observation horizon of 1 and an action prediction horizon of 20. We take advantage of noise scheduler decoupling, using 100 denoising steps during training and 10 steps at inference. At inference, we execute 8 of the 20 predicted actions.

### C. Data Collection

The expert demonstrations used to train our tactile imitation learning framework were collected via teleoperation of a Franka Emika Panda robot. We used the Oculus Virtual Reality (VR) teleoperation pipeline developed by [67], which tracks the Quest’s controller using the headset. However, we

did not use VR for observing the tasks, instead having the operators directly look at the workspace. The teleoperation system provides a goal state (position and gripper width of the robot’s end effector) to an impedance controller, which controls the robot.

During teleoperation, six RGB views of the workspace were recorded using Realsense cameras, consisting of a D415 wrist-mounted camera, four D415 cameras mounted around the workspace, and a D445 camera mounted on the top edge of the workspace, which provided a scene overview. Additionally, the current state of the robot’s end-effector (x position, y position, z position, and gripper width) and the goal state (as measured by the teleoperation system) were recorded. The data collection system was run at 10 Hz. A view of the workspace can be seen in Figure 4.

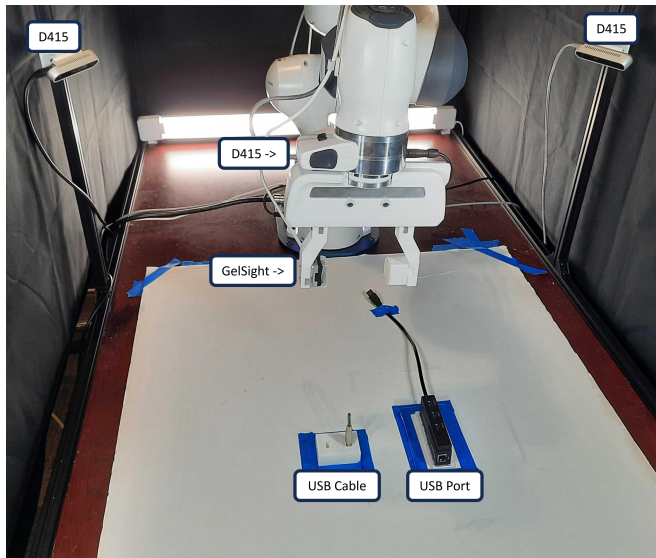


Fig. 4. Cable-Plugging workspace. A Franka Emika Panda robot retrieves the USB cable from its holder and plugs it into the front port on the USB hub. A GelSight captures tactile observations, while 6 Realsense D415 cameras observe the scene (only two can be seen above, with three out of view, and another mounted to the back of the end-effector).

Tactile observations were provided by a GelSight Mini, which was mounted to the robot’s end-effector. During our initial experimentation, we found that the high contact forces involved in cable plugging, along with the repetitive nature of data collection, led to significant wear on the soft silicon gel pad of the GelSight. A GelSight pad was only able to perform around 30 teleoperated cable plugging episodes before tearing. To address this issue, we equipped the GelSight with a 1 mm thick protective Ecoflex 00-50 silicon rubber topper. Although this topper reduced the GelSight’s ability to detect small-scale surface features, it preserved the GelSight’s perception of the large-scale features (contact pressure, contact area, strain, etc.) relevant to robotic manipulation tasks. A side-by-side comparison of the GelSight data with and without the protective cover can be seen in Figure 5. Despite the use of the cover, two additional GelSight pads were damaged during experimentation. However, the cover

managed to extend the lifetime of the GelSight pad by an order of magnitude, withstanding a few hundred plugging episodes before tearing.

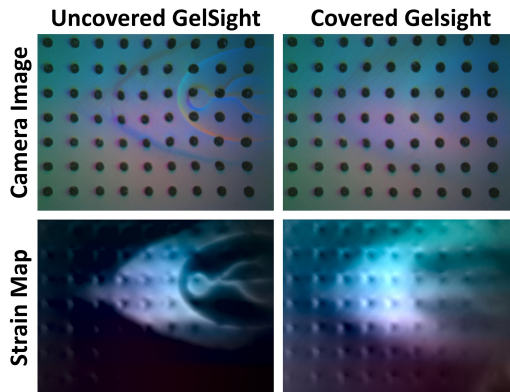


Fig. 5. GelSight sensor outputs. The top row shows RGB images from the GelSight’s camera. The bottom row shows the processed strain data, rendered in the LAB color space, with the brightness of each pixel corresponding to the normal strain (depth), and the color corresponding to the tangential strains, with strains in x shown on the blue-yellow spectrum, and strains in y shown on the red-green spectrum. The right column shows the outputs when the silicon gel cover is used, while the left column shows the uncovered outputs

Previous works using GelSight as a control policy input found that using processed data, such as strain information, out-performed directly using RGB images [68]. Based on these observations, and to reduce the impact of discrepancies between different GelSight pads, we used a processed tactile input for our imitation learning pipeline, representing the tactile information as a 240 x 320 map of the gel’s strain in the x, y, and z directions. A visualization of this strain data can be found in Figure 5.

#### IV. EXPERIMENTAL EVALUATION

We evaluated our model on the task of cable plugging. In this task, the robot has to navigate to a USB cable, unplug it from its holder, and plug it into the last port of a USB hub. We collected 100 demonstrations, with an average length of 208 time steps (approximately 21 seconds). Because we are most interested in the visuo-tactile task of inserting the USB cable, not the vision-only task of localizing the plug and cord, we fixed the start positions of the cord holder and USB plug. To increase the task’s difficulty, we added random noise to the agent’s actions during inference, sampled from  $\mathcal{N}(0, 2.5)$ mm. We then trained the agents on 80 demonstrations and reserved 20 for validation during the training process. We let the agents run until they successfully plugged in the cable, reached an un-recoverable state (ie. dropped the USB cable), or exceeded 300 time steps. All of our experiments were run 20 times. Due to wear on the original pad, a different gel pad was used during train and testing.

We ran 4 experiments per agent, comparing combined tactile and visual observations with only visual observations, evaluating both configurations with pretraining and without

pretraining. Additionally, we tested with only tactile observations (both with and without pretraining). Our results can be seen in Figure 6.

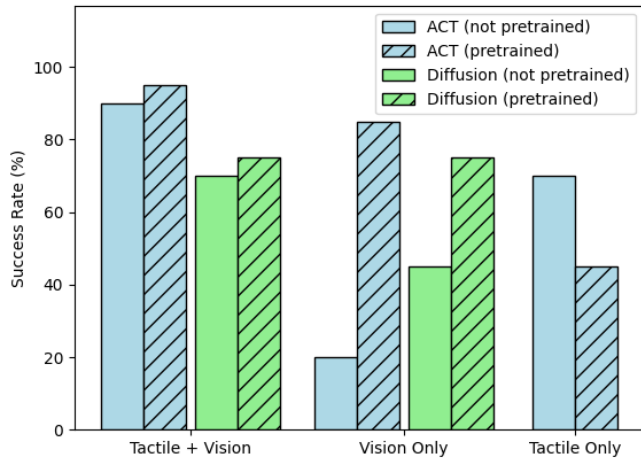


Fig. 6. Success rate for USB cable plugging. All experiments were run 20 times, with the total success rate shown. The use of visuo-tactile pretraining (hashed bars) leads to a slight increase in performance for visuo-tactile policies and a significant improvement for vision-only policies.

We found that by combining tactile observations with visual inputs, we were able to solve the cable plugging task, reaching a 95% success rate for ACT. This is significantly higher than the 20% and 45% success rates that learning from vision only with ACT and diffusion policy (respectively) achieves. Beyond solving the cable plugging task, our results show that contrastive pretraining results in a modest improvement in performance for both ACT and Diffusion Policy, granting both policies a 5% performance increase when used on the vision + tactile dataset. Although this is relatively small in absolute terms, it corresponds to a 50% and 20% decrease in failures for ACT and Diffusion Policy, respectively.

More importantly, pretraining with tactile data led to a significant improvement in the vision-only agent, increasing ACT’s performance from 20% to 85%, and diffusion policy’s from 45% to 75%, achieving almost the same level of performance as the visuo-tactile agent. In addition to improving overall performance, we found that pretraining with tactile information decreased the force exerted by the agent. We measured the mean absolute tangential strain at each timestep during execution, and examined the median across all runs, finding that pretraining reduced the strain in visuo-tactile policies by 8% and 13%, and by 20% and 17% in vision-only policies for ACT and Diffusion Policy, respectively.

Comparing our two imitation learning methods, we found that Diffusion Policy was less sensitive to changes in policy than ACT, with a higher accuracy for the non-pretrained vision only policy (where ACT did quite poorly), but lower accuracy for the pretrained vision and tactile+vision results (where ACT did quite well). Diffusion’s longer re-plan horizon (re-planning every 8 steps instead of every step)

and stochastic nature lead to larger motions, tending to jump around the port before plugging in the USB. These larger more random motions helped the policy avoid getting stuck (like ACT did) when poorly trained but impeded the well-trained policy. Also, the large more stochastic motions of Diffusion Policy caused an increase in contact force, with Diffusion Policy increasing GelSight strain by about 15% as compared to ACT for the pretrained visuo-tactile policy.

Finally, we evaluated the models without vision input (only tactile and positional data). Interestingly, the non-pretrained ACT model outperformed the pretrained model in this task. We think this may be due to overfitting, especially since we used different GelSight pads for training and evaluation. Diffusion Policy was unable to complete this task. For both pretrained and non-pretrained policies, the robot would pick up the USB cable, but then would alternate between trying to move back to the USB holder, trying to move towards the USB hub, and opening its gripper to re-grasp the USB (resulting in dropping the USB), never completing the task.

## V. CONCLUSIONS

In this work, we have shown that incorporating contrastive visuo-tactile pretraining into imitation learning frameworks can significantly boost agent performance in complex manipulation tasks, exemplified by USB cable plugging. By incorporating tactile information, we were able to achieve a 95% success rate on this task, a significant improvement from the 45% success rate we were able to achieve with vision only. Although much of this improvement came from the addition of tactile observations, our pretraining strategy had a positive impact, increasing our headline accuracy from 90% to 95%. Additionally, we found that pretraining decreased the force exerted by the agent, suggesting a more contact-aware policy.

Our most impactful finding was that by pretraining with tactile observations, we could significantly improve the performance of vision-only policies, allowing them to achieve a success rate on par with their visuo-tactile counterparts. This training paradigm could be especially useful in industrial applications, where durability and cost concerns limit the applicability of high-quality tactile sensors like GelSight. By using tactile observations only during the training phase, our method allows imitation learning policies to leverage tactile cues to significantly improve performance, without requiring the deployment of tactile sensors during operation.

A major limitation of this work is that task-specific data was used for pretraining. Although this strategy allowed the vision-only policy to learn the tactile features relevant to the specific task, it limits the applicability of the pretrained model and requires tactile observations to be collected for each task. An alternative approach would be to collect a large-scale visuo-tactile dataset for pretraining, then fine-tune a vision-only policy on a separate task, trading task-specific tactile knowledge for increased generalizability. Evaluating this alternative approach is left for future work.

## REFERENCES

- [1] M. Stenmark and J. Malec, "Knowledge-based instruction of manipulation tasks for industrial robotics," *Robotics and Computer-Integrated Manufacturing*, vol. 33, pp. 56–67, 2015.
- [2] A. Bartsch, C. Avra, and A. B. Farimani, "Sculptbot: Pre-trained models for 3d deformable object manipulation," *arXiv preprint arXiv:2309.08728*, 2023.
- [3] R. Johansson and J. Flanagan, "Tactile sensory control of object manipulation in humans," *The Senses: A Comprehensive Reference*, vol. 6, pp. 67–86, 01 2010.
- [4] K. Bark, E. Hyman, F. Tan, E. Cha, S. A. Jax, L. J. Buxbaum, and K. J. Kuchenbecker, "Effects of vibrotactile feedback on human learning of arm motions," *IEEE Transactions on Neural Systems and Rehabilitation Engineering*, vol. 23, no. 1, pp. 51–63, 2015.
- [5] W. Yuan, S. Dong, and E. H. Adelson, "Gelsight: High-resolution robot tactile sensors for estimating geometry and force," *Sensors*, vol. 17, no. 12, p. 2762, 2017.
- [6] Y. She, S. Wang, S. Dong, N. Sunil, A. Rodriguez, and E. Adelson, "Cable manipulation with a tactile-reactive gripper," *The International Journal of Robotics Research*, vol. 40, no. 12-14, pp. 1385–1401, 2021.
- [7] M. Kaboli, K. Yao, D. Feng, and G. Cheng, "Tactile-based active object discrimination and target object search in an unknown workspace," *Autonomous Robots*, vol. 43, pp. 123–152, 2019.
- [8] I. Guzey, B. Evans, S. Chintala, and L. Pinto, "Dexterity from touch: Self-supervised pre-training of tactile representations with robotic play," *arXiv preprint arXiv:2303.12076*, 2023.
- [9] T. Ablett, O. Limoyo, A. Sigal, A. Jilani, J. Kelly, K. Siddiqi, F. Hogan, and G. Dudek, "Push it to the demonstrated limit: Multimodal visuotactile imitation learning with force matching," *arXiv preprint arXiv:2311.01248*, 2023.
- [10] T. Z. Zhao, V. Kumar, S. Levine, and C. Finn, "Learning fine-grained bimanual manipulation with low-cost hardware," *arXiv preprint arXiv:2304.13705*, 2023.
- [11] C. Chi, S. Feng, Y. Du, Z. Xu, E. Cousineau, B. Burchfiel, and S. Song, "Diffusion policy: Visuomotor policy learning via action diffusion," *arXiv preprint arXiv:2303.04137*, 2023.
- [12] Q. Li, O. Kroemer, Z. Su, F. F. Veiga, M. Kaboli, and H. J. Ritter, "A review of tactile information: Perception and action through touch," *IEEE Transactions on Robotics*, vol. 36, no. 6, pp. 1619–1634, 2020.
- [13] C. Schurmann, R. Haschke, H. Ritter *et al.*, "A modular high-speed tactile sensor for human manipulation research," in *2011 IEEE World Haptics Conference*. IEEE, 2011, pp. 339–344.
- [14] Y. Zhang, "Sensitivity enhancement of a micro-scale biomimetic tactile sensor with epidermal ridges," *Journal of micromechanics and microengineering*, vol. 20, no. 8, p. 085012, 2010.
- [15] H. Liu, K. C. Nguyen, V. Perdereau, J. Bimbo, J. Back, M. Godden, L. D. Seneviratne, and K. Althoefer, "Finger contact sensing and the application in dexterous hand manipulation," *Autonomous Robots*, vol. 39, pp. 25–41, 2015.
- [16] T. P. Tomo, A. Schmitz, W. K. Wong, H. Kristanto, S. Somlor, J. Hwang, L. Jamone, and S. Sugano, "Covering a robot fingertip with uskin: A soft electronic skin with distributed 3-axis force sensitive elements for robot hands," *IEEE Robotics and Automation Letters*, vol. 3, no. 1, pp. 124–131, 2017.
- [17] B. Ward-Cherrier, N. Pestell, L. Cramphorn, B. Winstone, M. E. Giannaccini, J. Rossiter, and N. F. Lepora, "The tactip family: Soft optical tactile sensors with 3d-printed biomimetic morphologies," *Soft robotics*, vol. 5, no. 2, pp. 216–227, 2018.
- [18] G. De Maria, C. Natale, and S. Pirozzi, "Force/tactile sensor for robotic applications," *Sensors and Actuators A: Physical*, vol. 175, pp. 60–72, 2012.
- [19] G. Palli, C. Melchiorri, G. Vassura, U. Scarcia, L. Moriello, G. Berselli, A. Cavallo, G. De Maria, C. Natale, S. Pirozzi *et al.*, "The dexmart hand: Mechatronic design and experimental evaluation of synergy-based control for human-like grasping," *The International Journal of Robotics Research*, vol. 33, no. 5, pp. 799–824, 2014.
- [20] M. Meier, G. Walck, R. Haschke, and H. J. Ritter, "Distinguishing sliding from slipping during object pushing," in *2016 IEEE/RSJ International Conference on Intelligent Robots and Systems (IROS)*. IEEE, 2016, pp. 5579–5584.
- [21] G. Zöllner, V. Wall, and O. Brock, "Acoustic sensing for soft pneumatic actuators," in *2018 IEEE/RSJ International Conference on Intelligent Robots and Systems (IROS)*. IEEE, 2018, pp. 6986–6991.
- [22] D. Siegel, I. Garabieta, and J. Hollerbach, "An integrated tactile and thermal sensor," in *Proceedings. 1986 IEEE International Conference on Robotics and Automation*, vol. 3. IEEE, 1986, pp. 1286–1291.
- [23] J. Wade, T. Bhattacharjee, and C. C. Kemp, "A handheld device for the in situ acquisition of multimodal tactile sensing data," *arXiv preprint arXiv:1511.03152*, 2015.
- [24] T. Schlegl, M. Neumayer, S. Mühlbacher-Karrer, and H. Zangl, "A pre-touch sensing system for a robot grasper using magnetic and capacitive sensors," *IEEE Transactions on Instrumentation and Measurement*, vol. 62, no. 5, pp. 1299–1307, 2013.
- [25] D. Guo, P. Lancaster, L.-T. Jiang, F. Sun, and J. R. Smith, "Transmissive optical pretouch sensing for robotic grasping," in *2015 IEEE/RSJ International Conference on Intelligent Robots and Systems (IROS)*. IEEE, 2015, pp. 5891–5897.
- [26] Y. Ding, J. Bonse, R. Andre, and U. Thomas, "In-hand grasping pose estimation using particle filters in combination with haptic rendering models," *International Journal of Humanoid Robotics*, vol. 15, no. 01, p. 1850002, 2018.
- [27] S. Li, S. Lyu, and J. Trinkle, "State estimation for dynamic systems with intermittent contact," in *2015 IEEE International Conference on Robotics and Automation (ICRA)*. IEEE, 2015, pp. 3709–3715.
- [28] A. Petrovskaya, O. Khatib, S. Thrun, and A. Y. Ng, "Bayesian estimation for autonomous object manipulation based on tactile sensors," in *Proceedings 2006 IEEE International Conference on Robotics and Automation, 2006. ICRA 2006*. IEEE, 2006, pp. 707–714.
- [29] M. Kaboli, D. Feng, K. Yao, P. Lanillos, and G. Cheng, "A tactile-based framework for active object learning and discrimination using multimodal robotic skin," *IEEE Robotics and Automation Letters*, vol. 2, no. 4, pp. 2143–2150, 2017.
- [30] G. Vezzani, U. Pattacini, G. Battistelli, L. Chisci, and L. Natale, "Memory unscented particle filter for 6-dof tactile localization," *IEEE Transactions on Robotics*, vol. 33, no. 5, pp. 1139–1155, 2017.
- [31] K. Yao, M. Kaboli, and G. Cheng, "Tactile-based object center of mass exploration and discrimination," in *2017 IEEE-RAS 17th International Conference on Humanoid Robotics (Humanoids)*. IEEE, 2017, pp. 876–881.
- [32] M. Kaboli, K. Yao, and G. Cheng, "Tactile-based manipulation of deformable objects with dynamic center of mass," in *2016 IEEE-RAS 16th International Conference on Humanoid Robots (Humanoids)*. IEEE, 2016, pp. 752–757.
- [33] W. K. Do and M. Kennedy, "Densetact: Optical tactile sensor for dense shape reconstruction," in *2022 International Conference on Robotics and Automation (ICRA)*. IEEE, 2022, pp. 6188–6194.
- [34] W. K. Do, B. Jurewicz, and M. Kennedy, "Densetact 2.0: Optical tactile sensor for shape and force reconstruction," in *2023 IEEE International Conference on Robotics and Automation (ICRA)*. IEEE, 2023, pp. 12 549–12 555.
- [35] W. K. Do, A. K. Dhawan, M. Kitzmann, and M. Kennedy III, "Densetact-mini: An optical tactile sensor for grasping multi-scale objects from flat surfaces," *arXiv preprint arXiv:2309.08860*, 2023.
- [36] F. R. Hogan, M. Jenkin, S. Rezaei-Shoshtari, Y. Girdhar, D. Meger, and G. Dudek, "Seeing through your skin: Recognizing objects with a novel visuotactile sensor," in *Proceedings of the IEEE/CVF Winter Conference on Applications of Computer Vision*, 2021, pp. 1218–1227.
- [37] W. Yuan, R. Li, M. A. Srinivasan, and E. H. Adelson, "Measurement of shear and slip with a gelsight tactile sensor," in *2015 IEEE International Conference on Robotics and Automation (ICRA)*. IEEE, 2015, pp. 304–311.
- [38] A. Wilson, H. Jiang, W. Lian, and W. Yuan, "Cable routing and assembly using tactile-driven motion primitives," in *2023 IEEE International Conference on Robotics and Automation (ICRA)*. IEEE, 2023, pp. 10 408–10 414.
- [39] G. Palli and S. Pirozzi, "A tactile-based wire manipulation system for manufacturing applications," *Robotics*, vol. 8, no. 2, p. 46, 2019.
- [40] C. Sferazza, Y. Seo, H. Liu, Y. Lee, and P. Abbeel, "The power of the senses: Generalizable manipulation from vision and touch through masked multimodal learning," 2023.
- [41] Y. Chen, M. Van der Merwe, A. Sipos, and N. Fazeli, "Visuo-tactile transformers for manipulation," in *6th Annual Conference on Robot Learning*, 2022.
- [42] W. Yang, A. Angleraud, R. S. Pieters, J. Pajarinen, and J.-K. Kämäräinen, "Seq2seq imitation learning for tactile feedback-based manipulation," in *2023 IEEE International Conference on Robotics and Automation (ICRA)*. IEEE, 2023, pp. 5829–5836.

- [43] J. Pari, N. M. Shafiqullah, S. P. Arunachalam, and L. Pinto, "The surprising effectiveness of representation learning for visual imitation," *arXiv preprint arXiv:2112.01511*, 2021.
- [44] K. Yu, Y. Han, M. Zhu, and Y. Zhao, "Mimictouch: Learning human's control strategy with multi-modal tactile feedback," *arXiv preprint arXiv:2310.16917*, 2023.
- [45] N. Rethmeier and I. Augenstein, "A primer on contrastive pretraining in language processing: Methods, lessons learned, and perspectives," *ACM Computing Surveys*, vol. 55, no. 10, pp. 1–17, 2023.
- [46] T. Chen, S. Kornblith, M. Norouzi, and G. Hinton, "A simple framework for contrastive learning of visual representations," in *International conference on machine learning*. PMLR, 2020, pp. 1597–1607.
- [47] K. Meidani, P. Shojaei, C. K. Reddy, and A. B. Farimani, "Snip: Bridging mathematical symbolic and numeric realms with unified pre-training," *arXiv preprint arXiv:2310.02227*, 2023.
- [48] Y. Wang, J. Wang, Z. Cao, and A. Barati Farimani, "Molecular contrastive learning of representations via graph neural networks," *Nature Machine Intelligence*, vol. 4, no. 3, pp. 279–287, 2022.
- [49] C. Lorusso and A. B. Farimani, "Picl: Physics informed contrastive learning for partial differential equations," *arXiv preprint arXiv:2401.16327*, 2024.
- [50] A. Radford, J. W. Kim, C. Hallacy, A. Ramesh, G. Goh, S. Agarwal, G. Sastry, A. Askell, P. Mishkin, J. Clark *et al.*, "Learning transferable visual models from natural language supervision," in *International conference on machine learning*. PMLR, 2021, pp. 8748–8763.
- [51] J. Kerr, H. Huang, A. Wilcox, R. Hoque, J. Ichnowski, R. Calandra, and K. Goldberg, "Self-supervised visuo-tactile pretraining to locate and follow garment features," *arXiv preprint arXiv:2209.13042*, 2022.
- [52] M. Zambelli, Y. Aytar, F. Visin, Y. Zhou, and R. Hadsell, "Learning rich touch representations through cross-modal self-supervision," in *Conference on Robot Learning*. PMLR, 2021, pp. 1415–1425.
- [53] V. Dave, F. Lygerakis, and E. Rueckert, "Multimodal visual-tactile representation learning through self-supervised contrastive pre-training," *arXiv preprint arXiv:2401.12024*, 2024.
- [54] D. A. Pomerleau, "Alvinn: An autonomous land vehicle in a neural network," *Advances in neural information processing systems*, vol. 1, 1988.
- [55] J. Ahn, M. Kim, and J. Park, "Autonomous driving using imitation learning with look ahead point for semi structured environments," *Scientific Reports*, vol. 12, no. 1, p. 21285, 2022.
- [56] J. Nakanishi, J. Morimoto, G. Endo, G. Cheng, S. Schaal, and M. Kawato, "Learning from demonstration and adaptation of biped locomotion," *Robotics and autonomous systems*, vol. 47, no. 2-3, pp. 79–91, 2004.
- [57] A. George and A. B. Farimani, "One act play: Single demonstration behavior cloning with action chunking transformers," *arXiv preprint arXiv:2309.10175*, 2023.
- [58] N. M. Shafiqullah, Z. Cui, A. A. Altanzaya, and L. Pinto, "Behavior transformers: Cloning  $k$  modes with one stone," *Advances in neural information processing systems*, vol. 35, pp. 22955–22968, 2022.
- [59] A. Hussein, M. M. Gaber, E. Elyan, and C. Jayne, "Imitation learning: A survey of learning methods," *ACM Computing Surveys (CSUR)*, vol. 50, no. 2, pp. 1–35, 2017.
- [60] J. Ho, A. Jain, and P. Abbeel, "Denoising diffusion probabilistic models," *arXiv preprint arxiv:2006.11239*, 2020.
- [61] M. Janner, Y. Du, J. Tenenbaum, and S. Levine, "Planning with diffusion for flexible behavior synthesis," in *International Conference on Machine Learning*, 2022.
- [62] E. Perez, F. Strub, H. De Vries, V. Dumoulin, and A. Courville, "Film: Visual reasoning with a general conditioning layer," in *Proceedings of the AAAI conference on artificial intelligence*, vol. 32, no. 1, 2018.
- [63] Z. Wang, J. J. Hunt, and M. Zhou, "Diffusion policies as an expressive policy class for offline reinforcement learning," *arXiv preprint arXiv:2208.06193*, 2022.
- [64] C. Lu, P. Ball, Y. W. Teh, and J. Parker-Holder, "Synthetic experience replay," *Advances in Neural Information Processing Systems*, vol. 36, 2024.
- [65] S. Sinha, A. Mandlekar, and A. Garg, "S4rl: Surprisingly simple self-supervision for offline reinforcement learning in robotics," in *Conference on Robot Learning*. PMLR, 2022, pp. 907–917.
- [66] K. He, X. Zhang, S. Ren, and J. Sun, "Deep residual learning for image recognition," in *Proceedings of the IEEE conference on computer vision and pattern recognition*, 2016, pp. 770–778.
- [67] A. George, A. Bartsch, and A. B. Farimani, "Openvr: Teleoperation for manipulation," *arXiv preprint arXiv:2305.09765*, 2023.
- [68] S. Dong, D. K. Jha, D. Romeres, S. Kim, D. Nikovski, and A. Rodriguez, "Tactile-rl for insertion: Generalization to objects of unknown geometry," in *2021 IEEE International Conference on Robotics and Automation (ICRA)*. IEEE, 2021, pp. 6437–6443.